

# A Photoionization Reflectron Time-of-Flight Mass Spectrometric Study on the Detection of Ethynamine (HCCNH<sub>2</sub>) and 2H-Azirine (c-H<sub>2</sub>CCHN)

Andrew M. Turner,<sup>[a, b]</sup> Sankhabrata Chandra,<sup>[a, b]</sup> Ryan C. Fortenberry,<sup>\*[c]</sup> and Ralf I. Kaiser<sup>\*[a, b]</sup>

Ices of acetylene (C<sub>2</sub>H<sub>2</sub>) and ammonia (NH<sub>3</sub>) were irradiated with energetic electrons to simulate interstellar ices processed by galactic cosmic rays in order to investigate the formation of C<sub>2</sub>H<sub>3</sub>N isomers. Supported by quantum chemical calculations, experiments detected product molecules as they sublime from the ices using photoionization reflectron time-of-flight mass spectrometry (PI-ReTOF-MS). Isotopically-labeled ices confirmed the C<sub>2</sub>H<sub>3</sub>N assignments while photon energies of 8.81 eV,

9.80 eV, and 10.49 eV were utilized to discriminate isomers based on their known ionization energies. Results indicate the formation of ethynamine (HCCNH<sub>2</sub>) and 2H-azirine (c-H<sub>2</sub>CCHN) in the irradiated C<sub>2</sub>H<sub>2</sub>:NH<sub>3</sub> ices, and the energetics of their formation mechanisms are discussed. These findings suggest that these two isomers can form in interstellar ices and, upon sublimation during the hot core phase, could be detected using radio astronomy.

## 1. Introduction

For the last decade, the elucidation of the fundamental reaction pathways leading to structural isomers – molecules with the same molecular formula, but distinct connectivities of atoms – of complex organic molecules (COMs) in the interstellar medium (ISM) has received considerable interest from the astrochemistry and physical chemistry communities.<sup>[1–3]</sup> This is because structural isomers have been recognized as tracers of physical and chemical conditions of, e.g., cold molecular clouds like TMC-1 and of star-forming regions like SgrB2, which are used to test chemical models through astrochemical modeling combined with astronomical observations.<sup>[4]</sup> Whereas considerable progress has been made toward a better understanding of the formation routes of COMs within carbon-, hydrogen-, and oxygen-bearing systems such as C<sub>3</sub>H<sub>6</sub>O [acetone (CH<sub>3</sub>COCH<sub>3</sub>), propanal (HCOCH<sub>2</sub>H<sub>5</sub>), propylene oxide (c-C<sub>3</sub>H<sub>6</sub>O)],<sup>[5]</sup> C<sub>2</sub>H<sub>6</sub>O<sub>2</sub> [ethylene glycol (HOCH<sub>2</sub>CH<sub>2</sub>OH), methoxymethanol (CH<sub>3</sub>OCH<sub>2</sub>OH)],<sup>[6]</sup> and C<sub>3</sub>H<sub>6</sub>O<sub>2</sub> [hydroxyacetone (CH<sub>3</sub>COCH<sub>2</sub>OH), ethyl formate (HCOOC<sub>2</sub>H<sub>5</sub>), methyl acetate (CH<sub>3</sub>COOCH<sub>3</sub>)] (Figure 1)<sup>[7]</sup> within the ices deposited on interstellar nanoparticles, few advances have been achieved with respect to structural isomers of carbon-, hydrogen-, and nitrogen-bearing systems. Structural isomers of C<sub>2</sub>H<sub>3</sub>N represent a peculiar problem. The

acetonitrile (CH<sub>3</sub>CN; 1) and methyl isocyanide (CH<sub>3</sub>NC; 2) 'isomer doublet' (Figure 2) – the methyl-substituted counterparts of hydrogen cyanide (HCN) and hydrogen isocyanide (HNC) – has been detected toward the star-forming region SgrB2.<sup>[4,8–9]</sup> However, none of their higher energy isomers has ever been identified in any astronomical environment: 2H-azirine (c-NCHCH<sub>2</sub>; 3),<sup>[10–14]</sup> ethynamine (HCCNH<sub>2</sub>; 4),<sup>[15–19]</sup> ketenimine (HNCCH<sub>2</sub>; 5),<sup>[20]</sup> or 1H-azirine (c-HNCHCH; 6).<sup>[21]</sup>

In terrestrial laboratories, 2H-azirine (c-NCHCH<sub>2</sub>; 3) may act both as a nucleophile as well as an electrophile,<sup>[22–25]</sup> therefore, its derivatives have been exploited in preparative organic chemistry<sup>[23,26–27]</sup> toward the synthesis of heterocyclic rings,<sup>[24]</sup> Diels-Alder reactions,<sup>[28]</sup> and photochemically-activated reactions.<sup>[9,29]</sup> The gas phase preparation of 3 was accomplished via pyrolysis of vinyl azide<sup>[30]</sup> and 1H-1,2,3-triazole,<sup>[31]</sup> in addition, 3 was matrix-isolated and tentatively identified via infrared spectroscopy by exposing 1 to laser-ablated transition metals.<sup>[32]</sup> Crossed molecular beam experiments along with statistical calculations on the possible identification of 3 yielded conflicting results.<sup>[33–34]</sup> The preparation of 4, which is an amino (-NH<sub>2</sub>) substituted acetylene molecule, was first reported in 1988 through vacuum pyrolysis of the keto and amine derivative of isoxazole (c-H<sub>3</sub>C<sub>3</sub>NO),<sup>[35]</sup> whereas 5 was observed through photolysis of hydrazoic acid (HN<sub>3</sub>) in the presence of acetylene (C<sub>2</sub>H<sub>2</sub>). This isomer has been exploited in preparative organic synthesis involving nucleophilic additions, radical additions, cycloaddition reactions, electrocyclic ring closure reactions, and  $\sigma$  rearrangements.<sup>[36]</sup> The thermodynamically least stable isomer 6 has not been prepared to date.

In this work, the preparation and detection of 2H-azirine (c-NCHCH<sub>2</sub>; 3) along with ethynamine (HCCNH<sub>2</sub>; 4) by exposing low-temperature ices of acetylene (C<sub>2</sub>H<sub>2</sub>) and ammonia (NH<sub>3</sub>) along with their isotopically substituted counterparts (<sup>13</sup>C<sub>2</sub>H<sub>2</sub>:NH<sub>3</sub>, C<sub>2</sub>H<sub>2</sub>:<sup>15</sup>NH<sub>3</sub>, <sup>13</sup>C<sub>2</sub>H<sub>2</sub>:<sup>15</sup>NH<sub>3</sub>, C<sub>2</sub>D<sub>2</sub>:NH<sub>3</sub>) to energetic electrons is reported. The neutral molecules formed are then sublimed into the gas phase, ionized according to their distinct

[a] Dr. A. M. Turner, Dr. S. Chandra, Prof. Dr. R. I. Kaiser  
Department of Chemistry, University of Hawaii at Manoa, 2545 McCarthy Mall, Honolulu, HI 96822 (USA)  
E-mail: ralfk@hawaii.edu

[b] Dr. A. M. Turner, Dr. S. Chandra, Prof. Dr. R. I. Kaiser  
W. M. Keck Laboratory in Astrochemistry, University of Hawaii at Manoa, 2545 McCarthy Mall, Honolulu, HI 96822 (USA)

[c] Prof. R. C. Fortenberry  
Department of Chemistry & Biochemistry, University of Mississippi, Mississippi 38677-1848 (USA)  
E-mail: r410@olemiss.edu

Supporting information for this article is available on the WWW under <https://doi.org/10.1002/cphc.202100064>

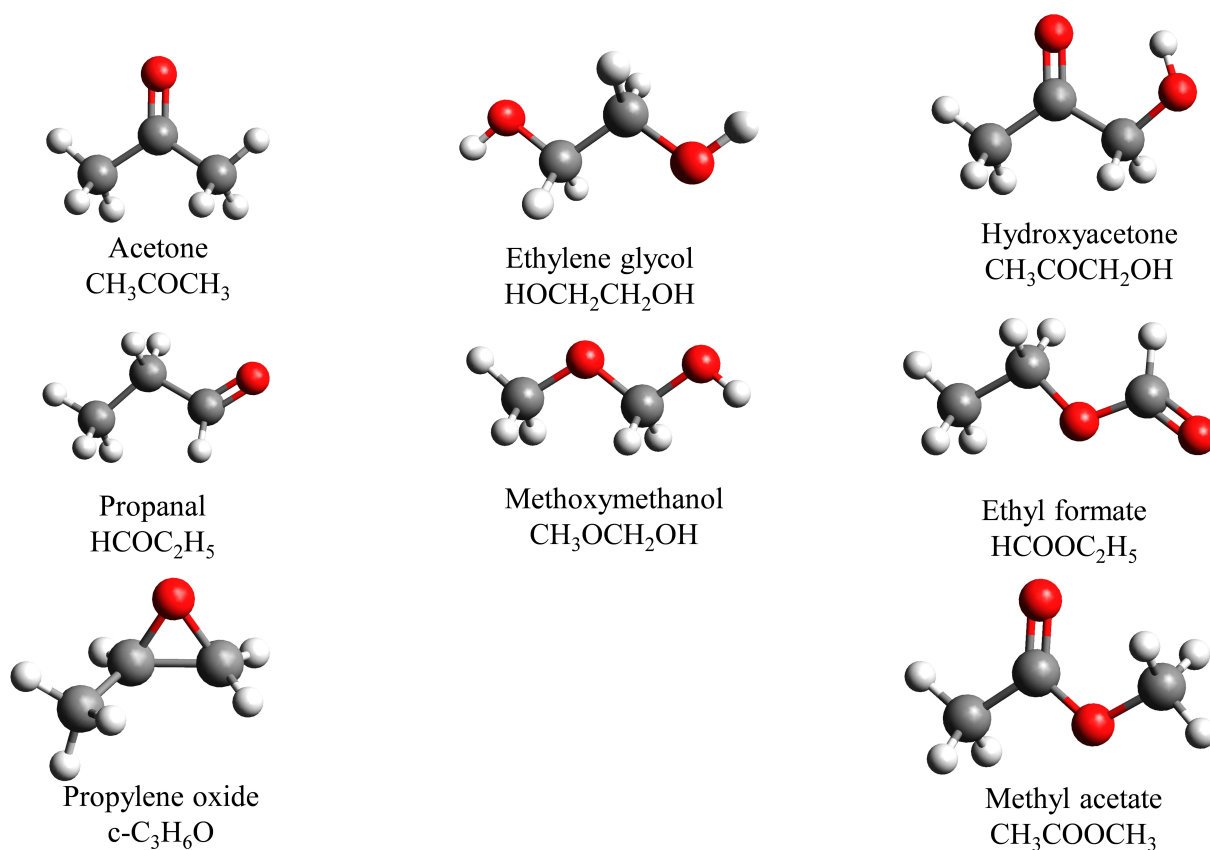


Figure 1. Selected key classes of complex organic molecules (COMs) within the carbon, hydrogen, and oxygen system.

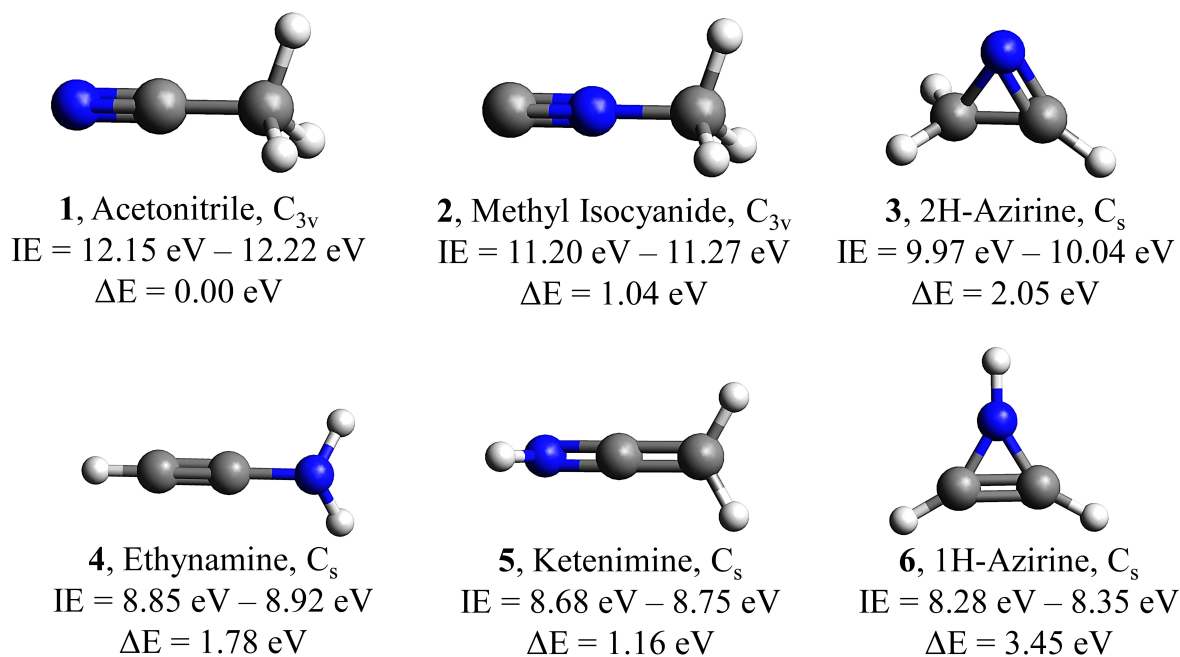


Figure 2. Isomers of  $\text{C}_2\text{H}_3\text{N}$  are shown in the sequence of decreasing adiabatic ionization energies. CCSD(T)/CBS + ZPVE adiabatic ionization energies are corrected by incorporating the error analysis (Table S9). Relative energies and point groups of each isomer are also shown.

adiabatic ionization energies by single photon ionization (PI) using vacuum ultraviolet (VUV) photons, and subsequently mass resolved and detected within a reflectron time-of-flight mass spectrometer (ReTOF-MS).<sup>[37–38]</sup> Discrete photon energies of 10.49 eV, 9.80 eV, and 8.81 eV along with isotopic substitution experiments were exploited to determine the molecular formula of the products, to discriminate between structural isomers, and to infer in combination with electronic structure calculations possible reaction pathways to their formation. Although acetylene has not been identified on interstellar ices, laboratory studies provide explicit evidence that acetylene represents a major reaction product of the radiolysis and photolysis of methane (CH<sub>4</sub>) ices,<sup>[39–41]</sup> which has been detected on interstellar grains at levels of up to 6%.<sup>[42]</sup> Along with ammonia, present at levels of up to 10%, in interstellar ices<sup>[42–44]</sup> and also observed, e.g., on moons of Saturn (Enceladus), Uranus (Miranda), and Pluto (Charon)<sup>[45–49]</sup> as well as the Kuiper Belt Object Quaoar,<sup>[50]</sup> both 3 and 4 are expected to be formed in interstellar ices. In the hot-core stage, sublimation drives the newly formed molecules into the gas phase, where they might be detected with radio telescopes such as the Atacama Large Millimeter/submillimeter Array (ALMA) thus providing a better understanding on the intrinsic formation pathways of structural isomers within the carbon-, hydrogen-, and nitrogen-bearing system.

## Experimental Methods

The experiments were performed in a contamination-free ultrahigh vacuum (UHV) stainless steel surface science chamber operated at pressures of a few 10<sup>-11</sup> Torr exploiting magnetically suspended turbomolecular pumps coupled with oil-free scroll backing pumps.<sup>[39,51]</sup> In brief, a silver substrate was interfaced to a two-stage closed-cycle helium cryostat (Sumitomo Heavy Industries, RDK-415E) that can be freely rotated and translated vertically. After cooling the substrate to 4.6 ± 0.1 K, acetylene (C<sub>2</sub>H<sub>2</sub>; 99.9%, Airgas) and ammonia (NH<sub>3</sub>; 99.999%, Matheson) were simultaneously introduced into the main chamber via a pair of glass capillary arrays at a pressure of 2 × 10<sup>-8</sup> Torr and deposited onto the substrate. Traces of acetone in the acetylene were removed by a dry ice-ethanol slush bath. Laser interferometry was used to determine the total ice thickness with a helium-neon (HeNe) laser operating at 632.8 nm.<sup>[52–53]</sup> Considering the refractive index of the ices of 1.36 ± 0.02,<sup>[54–55]</sup> a thickness of 1,000 ± 100 nm was derived. The ice ratio of acetylene to ammonia was determined to be 1:1 ± 0.2 by accounting for the integrated absorption coefficients of the ν<sub>5</sub> mode at 746 cm<sup>-1</sup> (2.4 × 10<sup>-17</sup> cm molecule<sup>-1</sup>) and the ν<sub>3</sub> mode at 3239 cm<sup>-1</sup> (2.4 × 10<sup>-17</sup> cm molecule<sup>-1</sup>) for acetylene<sup>[56]</sup> along with the ν<sub>2</sub> mode at 1077 cm<sup>-1</sup> (2.1 × 10<sup>-17</sup> cm molecule<sup>-1</sup>), ν<sub>4</sub> mode at 1627 cm<sup>-1</sup> (5.6 × 10<sup>-18</sup> cm molecule<sup>-1</sup>) and ν<sub>3</sub> mode at 3394 cm<sup>-1</sup> (2.3 × 10<sup>-17</sup> cm molecule<sup>-1</sup>) for ammonia.<sup>[57]</sup> The ices were then irradiated at 4.6 ± 0.1 K for 60 minutes with 5 keV electrons at a current of 100 nA scanned over an area of 1.0 ± 0.1 cm<sup>2</sup> at an angle of incidence of 70° relative to the surface normal (Table S1). An average penetration depth of the energetic electrons was computed via Monte Carlo simulations (CASINO)<sup>[58]</sup> to be 350 ± 30 nm (Table S2). Since the maximum penetration depth (700 ± 50 nm) is less than the thickness of the deposited ices, the energetic electrons only interact with the ices, but not with the substrate. On average, the dose is calculated to be 5.0 ± 0.8 eV per C<sub>2</sub>H<sub>2</sub> and 3.5 ± 0.6 eV per NH<sub>3</sub> molecule (Table S1). During the electron irradiation,

the ices were monitored with a Fourier-transform infrared spectrometer (FTIR, Nicolet 6700) in the range of 4000 cm<sup>-1</sup> to 700 cm<sup>-1</sup> at 4 cm<sup>-1</sup> resolution averaging spectra over 2 minutes, i.e. up to 30 accumulated spectra in total during the irradiation. After the electron irradiation, temperature programmed desorption (TPD) was performed to sublime the ices along with the newly formed products. Each exposed sample was heated from 5 K to 300 K at a rate of 1 K min<sup>-1</sup>. During TPD, a reflectron time-of-flight mass spectrometer (ReTOF-MS, Jordan TOF Products, Inc.) coupled with photoionization (PI) at photon energies of 10.49 eV, 9.80 eV and 8.81 eV was utilized to ionize the subliming molecules. To generate these photon energies, pulsed (30 Hz) coherent vacuum ultraviolet (VUV) light was generated via four-wave mixing using krypton (Specialty Gases, 99.999%) or xenon (Specialty Gases, 99.999%) as a nonlinear medium (Table S3). The VUV light was separated from the fundamentals using a lithium fluoride (LiF) biconvex lens<sup>[59]</sup> (ISP Optics) based on distinct refractive indices of the lens material for different wavelengths.<sup>[60]</sup> The photoionized molecules were extracted, and mass-to-charge ratios were determined on the basis of the arrival time of the ions at a multichannel plate. The signal was amplified with a fast preamplifier (Ortec 9305) and recorded using a bin width of 4 ns that was triggered at 30 Hz (Quantum Composers, 9518). Infrared and PI-ReTOF-MS assignments were cross checked and verified with ices containing isotopically substituted counterparts such as <sup>13</sup>C<sub>2</sub>H<sub>2</sub>:NH<sub>3</sub> (<sup>13</sup>C<sub>2</sub>H<sub>2</sub>; > 99 % <sup>13</sup>C, Cambridge Isotope), C<sub>2</sub>H<sub>2</sub>:<sup>15</sup>NH<sub>3</sub> (<sup>15</sup>NH<sub>3</sub>; > 98 % <sup>15</sup>N, Sigma Aldrich), <sup>13</sup>C<sub>2</sub>H<sub>2</sub>:<sup>15</sup>NH<sub>3</sub>, and C<sub>2</sub>D<sub>2</sub>:NH<sub>3</sub> (C<sub>2</sub>D<sub>2</sub>; > 99 % D, C/D/N Isotope)

## Computational Details

The quantum chemical computations rely upon the CCSD(T) method<sup>[61]</sup> and the aug-cc-pVTZ basis set<sup>[62–63]</sup> in large part. The minimum energy geometries are optimized and subsequent harmonic frequencies are computed at this level of theory for the minima on the potential energy surface (PES). The energies reported, however, are based on 2-point complete basis set (CBS) limit extrapolations<sup>[64]</sup> for the optimized CCSD(T)/aug-cc-pVTZ energy and a single-point CCSD(T)/aug-cc-pVQZ energy at the optimized CCSD(T)/aug-cc-pVTZ geometry. This energy is then corrected for zero-point vibrational energy (ZPVE) from the optimized CCSD(T)/aug-cc-pVTZ geometry. The transition states (TS) are optimized and frequencies computed with B3LYP<sup>[65–67]</sup> again with the aug-cc-pVTZ basis set, but the energies are CCSD(T)/aug-cc-pVTZ and aug-cc-pVQZ single-point CBS energies with B3LYP/aug-cc-pVTZ ZPVE energies. Dissociation of hydrogen atoms is computed via a relaxed CCSD(T)/aug-cc-pVTZ scan of the dissociation coordinate. Similar scans also produce the association of acetylene (C<sub>2</sub>H<sub>2</sub>) with the amino radical (NH<sub>2</sub>) via a relaxed scan of a C–N bond, and scans of the major reaction coordinates support the TS assignments. All energies on the reported PES are relative to the C<sub>2</sub>H<sub>2</sub> and NH<sub>2</sub> reactants unless otherwise noted. The reported coupled cluster results utilize the Molpro2015.1 quantum chemistry program,<sup>[68–69]</sup> and the B3LYP results utilize the Gaussian09 quantum chemistry program.<sup>[70]</sup> Molecular coordinates and harmonic frequencies are provided in the Supporting Information.

## 2. Results and Discussion

### 2.1. Computational

Previous work by Dickerson, et al.<sup>[14]</sup> examined similar portions of the [C, N, H<sub>4</sub>] PES. Their CCSD(T)/cc-pV5Z isomerization energy between the 1-H and 2-H azirines is 140.2 kJ mol<sup>-1</sup>, while

the present is  $135.2 \text{ kJ mol}^{-1}$ , which suggests that the present results are reliable. They further compute a  $499.2 \text{ kJ mol}^{-1}$  transition state barrier beginning from 2-H azirine between the two azirine isomers with  $\omega\text{B97-X/cc-pVTZ}$ , while the present one is  $242.9 \text{ kJ mol}^{-1}$ . However, the present transition state has the correct behavior for the imaginary frequency, utilizes higher levels of theory, and produces a lower barrier lending credence to the reliability of the present results over the previous. Additionally, conformers (7) and (8) are analyzed, and the trans forms are lower in energy than the cis forms by  $6 \text{ kJ mol}^{-1}$  and  $2 \text{ kJ mol}^{-1}$ , respectively, with barriers between the cis/trans forms of  $16 \text{ kJ mol}^{-1}$  and  $69 \text{ kJ mol}^{-1}$ , respectively. The rest of this discussion will be limited to these two trans forms for simplicity and since these two forms are the most likely to take part in the reactions.

## 2.2. Infrared Spectroscopy

Figure 3 displays the FTIR spectra of the acetylene-ammonia ice before and after the irradiation. Overall, both spectra are dominated by the fundamentals of acetylene ( $\nu_5$ ,  $746 \text{ cm}^{-1}$ ;  $\nu_2$ ,  $1950 \text{ cm}^{-1}$ ) and ammonia ( $\nu_2$ ,  $1077 \text{ cm}^{-1}$ ;  $\nu_4$ ,  $1627 \text{ cm}^{-1}$ ;  $\nu_1$ ,  $3187 \text{ cm}^{-1}$ ;  $\nu_3$ ,  $3394 \text{ cm}^{-1}$ ) along with their combination modes and overtones for acetylene ( $\nu_4 + \nu_5$ ,  $1389 \text{ cm}^{-1}$ ) and ammonia ( $2\nu_4$ ,  $3303 \text{ cm}^{-1}$ ). After the irradiation, new peaks emerged including the CH deformation mode at  $962 \text{ cm}^{-1}$ , CH stretching modes at  $2801 \text{ cm}^{-1}$  and  $2973 \text{ cm}^{-1}$ , deformation of primary amines ( $\text{RNH}_2$ ) at  $1594 \text{ cm}^{-1}$ , and CCN stretching at  $2054 \text{ cm}^{-1}$  (Table S4). The FTIR spectra for isotopically labelled ices ( $^{13}\text{C}_2\text{H}_2:\text{NH}_3$ ,  $\text{C}_2\text{H}_2:^{15}\text{NH}_3$ ,  $^{13}\text{C}_2\text{H}_2:^{15}\text{NH}_3$ ,  $\text{C}_2\text{D}_2:\text{NH}_3$ ) before and after irradiation are shown in Figure S1–S4 along with newly obtained peaks (Tables S5–S8). The aforementioned assignments could be verified via the absorptions in, e.g., the  $^{13}\text{C}_2\text{H}_2:\text{NH}_3$  ice:  $\nu_5$  ( $745 \text{ cm}^{-1}$ ) and  $\nu_2$  ( $1887 \text{ cm}^{-1}$ ) for acetylene and  $\nu_2$  ( $1075 \text{ cm}^{-1}$ ),  $\nu_4$  ( $1628 \text{ cm}^{-1}$ ),  $\nu_1$  ( $3175 \text{ cm}^{-1}$ ), and  $\nu_3$  ( $3397 \text{ cm}^{-1}$ ) for ammonia.

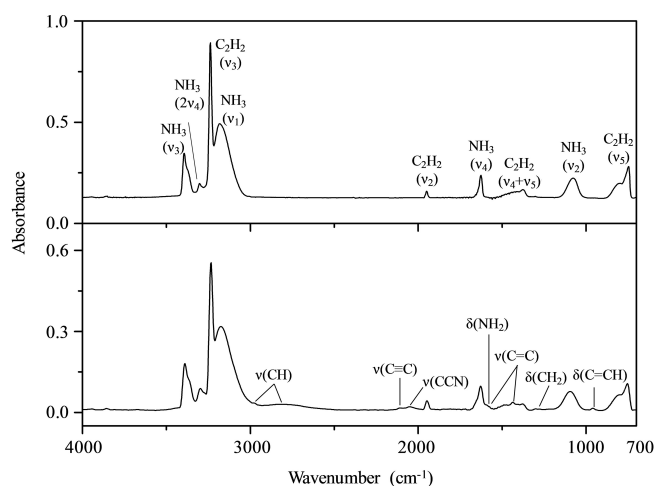


**Figure 3.** Infrared spectra for the  $\text{C}_2\text{H}_2:\text{NH}_3$  ice before (top) and after (bottom) electron irradiation of 100 nA for 60 minutes. New absorption bands from irradiation are labeled in the bottom spectrum. Absorptions are compiled in Table S4.

However, due to the complexity of the new molecules formed, infrared data only provide information of the *functional groups* of the newly formed molecules.<sup>[37,51]</sup> Therefore, *individual molecules* formed in these ices cannot be identified from the FTIR spectra. Therefore, an alternative analytical approach is required to isomer-selectively assign newly formed molecules.

## 2.3. Photoionization Reflectron Time-of-Flight Mass Spectrometry (PI-ReTOF-MS)

To identify *individual molecules* prepared during the exposure of the acetylene-ammonia ices to ionizing radiation, photoionization reflectron time-of-flight mass spectrometry (PI-ReTOF-MS) was exploited during the TPD phase. This method represents a unique isomer-selective approach of photoionizing and discriminating molecules in the gas phase based on distinct adiabatic ionization energies (IE) of structural isomers (Figure 2, Table S9) by systematically tuning the photon energies above and below the IE of the isomer(s) of interest.<sup>[2,51,71]</sup> The sublimation profiles report the ion counts versus temperature of distinctive mass-to-charge ratios ( $m/z$ ) (Figure 4).

At a photon energy of 10.49 eV, the ReTOF-MS data are dominated by the molecular ion peaks of ammonia at  $m/z = 17$  ( $\text{NH}_3^+$ ) and 18 ( $^{15}\text{NH}_3^+$ ) (IE = 10.07 eV) (Figure 4). A comparison of the data of the pristine ices with the irradiated ices uncovers the formation of new molecules. The temperature programmed desorption (TPD) profile of the  $\text{C}_2\text{H}_2:\text{NH}_3$  system reveals prominent ion counts at  $m/z = 41$  at a photon energy of 10.49 eV with distinct peaks at 105 K (green), 160 K (red), and 200 K (blue) (Figure 5), hereafter referred to peak I, II, and III, respectively. To assign peak I, an inspection of the TPD at  $m/z = 40$  is required (Figure S5). The highlighted peak at  $m/z = 40$  can be associated with  $\text{C}_3\text{H}_4$  (allene, methylacetylene). This position matches peak I for  $m/z = 41$ . The integrated ion counts at  $m/z = 41$  are detected at levels of  $3.2 \pm 0.3\%$  compared to  $m/z = 40$ , suggesting that peak I is linked to  $^{13}\text{CC}_2\text{H}_4$  given the natural isotopic abundance of carbon-13 of 1.1%. This is also confirmed in isotopic studies. Here, since ion counts at  $m/z = 41$  cannot be only connected to  $\text{C}_2\text{H}_3\text{N}^+$ , but also to  $^{13}\text{CC}_2\text{H}_4$  (allene, methylacetylene), the products formed in the isotopically labelled ices along with their mass shifts upon labeling must be considered (Figure 6). In the  $\text{C}_2\text{H}_2:^{15}\text{NH}_3$  system, three sublimation events are also present at  $m/z = 42$ . The early event can be linked to  $\text{C}_3\text{H}_6$  isomers propylene and/or cyclopropane, and this peak shifts to  $m/z = 45$  upon  $^{13}\text{C}$  substitution revealing that this molecule carries three carbon-13 atoms (39 amu) and six hydrogen atoms (6 amu) (Figure S6); further, the sublimation temperature of 105 K of this peak agrees well with previous sublimation temperatures of propylene and/or cyclopropane in pure hydrocarbon systems.<sup>[56]</sup> Peaks II and III can be linked to  $\text{C}_2\text{H}_3^{15}\text{N}$  ( $m/z = 42$ ) as these shift by one amu compared to the  $\text{C}_2\text{H}_2:\text{NH}_3$  system. Therefore, the isomer(s) at both higher temperature sublimation profiles have one nitrogen atom. Further, in the  $^{13}\text{C}_2\text{H}_2:\text{NH}_3$  system, three sublimation events are visible as well for  $m/z = 43$  at 105 K, 160 K, and 200 K. The first peak can be accounted for by  $^{13}\text{C}_3\text{H}_4$  (allene, methylacetylene)

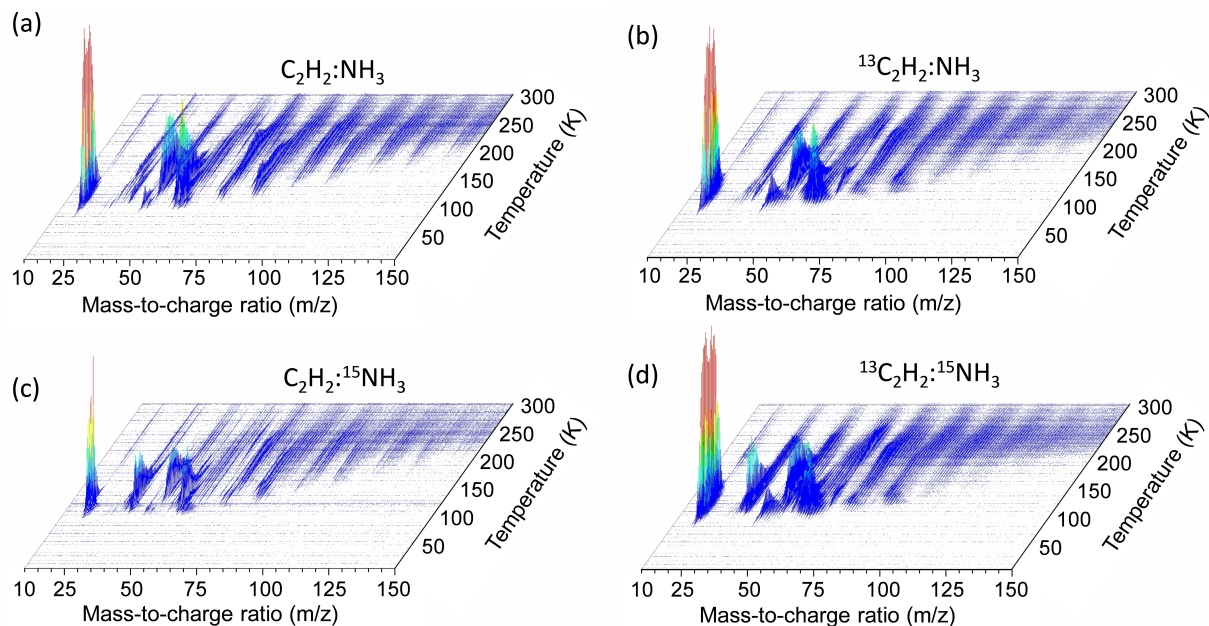


Figure 4. PI-ReTOF-MS data recorded for irradiated (a)  $\text{C}_2\text{H}_2:\text{NH}_3$ , (b)  $^{13}\text{C}_2\text{H}_2:\text{NH}_3$ , (c)  $\text{C}_2\text{H}_2:^{15}\text{NH}_3$ , and (d)  $^{13}\text{C}_2\text{H}_2:^{15}\text{NH}_3$  ices at a photon energy of 10.49 eV.

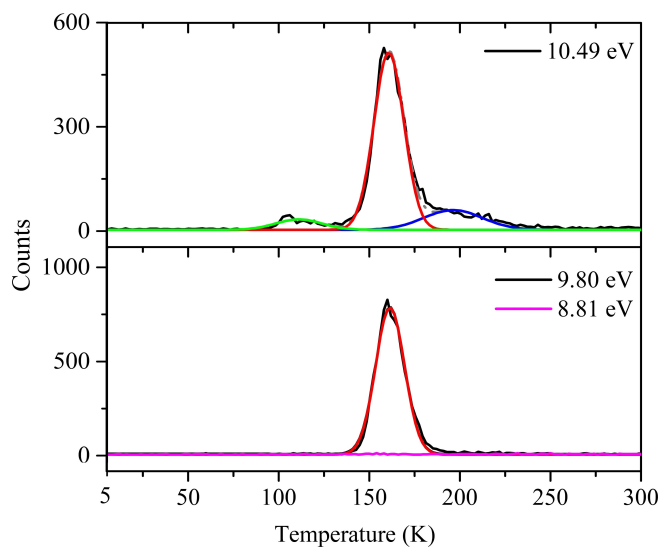


Figure 5. Temperature-programmed desorption profiles of the ionized neutral molecules for  $m/z = 41$  subliming from  $\text{C}_2\text{H}_2:\text{NH}_3$  ices at photon energies of 10.49 eV (top, black), 9.80 eV (bottom, black), and 8.81 eV (bottom, pink). The deconvoluted split Gaussian peaks (green, red and blue) and the fitted profiles (gray dashed) are also shown.

as this peak shifts to  $m/z = 40$  in the  $\text{C}_2\text{H}_2:\text{NH}_3$  system (Figure S5) indicating that this molecule holds three carbon-13 atoms (39 amu) plus four hydrogen atoms (4 amu). Peaks II and III represent the  $^{13}\text{C}_2\text{H}_3\text{N}$  isomers, which are shifted by 2 amu compared to the  $\text{C}_2\text{H}_3\text{N}$  formed in the  $\text{C}_2\text{H}_2:\text{NH}_3$  system. Therefore, peaks II and III at  $m/z = 41$  in the  $\text{C}_2\text{H}_2:\text{NH}_3$  system (Figure 5) can be linked to a molecule containing two carbon atoms, one nitrogen atom, and three hydrogen atoms, i.e. the

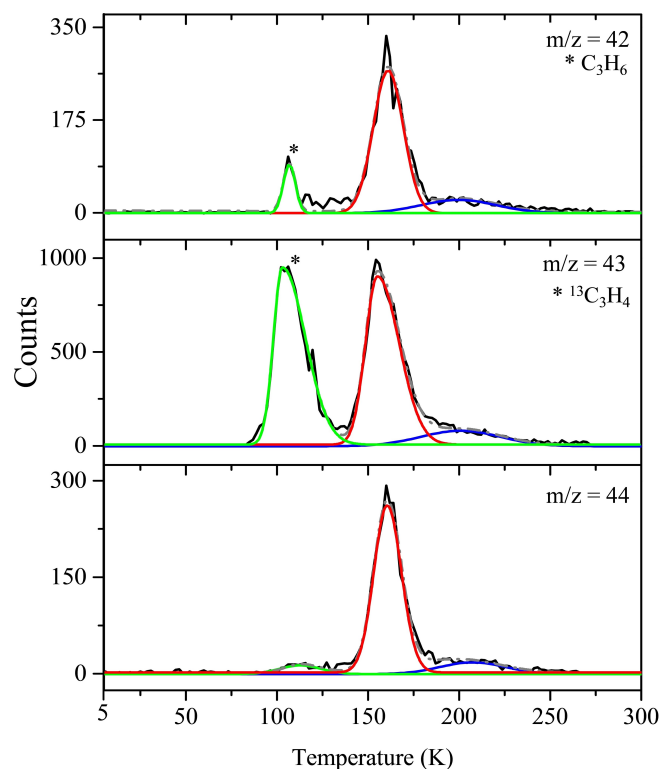


Figure 6. Temperature-programmed desorption profiles of the ionized neutral molecules at the indicated mass-to-charge ratios subliming from  $\text{C}_2\text{H}_2:^{15}\text{NH}_3$  (top),  $^{13}\text{C}_2\text{H}_2:\text{NH}_3$  (center), and  $^{13}\text{C}_2\text{H}_2:^{15}\text{NH}_3$  ices (bottom) at a photon energy 10.49 eV are shown. The deconvoluted split Gaussian peaks (green, red and blue) and the fitted profiles are also shown.

molecular formula  $C_2H_3N$ . To confirm these results, the TPD profile of  $m/z = 44$  in the  $^{13}C_2H_2: ^{15}NH_3$  system was also analyzed (Figure 6). The  $C_2H_3N$  isomers formed in the  $C_2H_2:NH_3$  ices should be shifted by 3 amu in the  $^{13}C_2H_2: ^{15}NH_3$  system, i.e. 2 amu for two  $^{13}C$  and one amu for one  $^{15}N$ . This is clearly confirmed through the appearance of peak II and III. Note that the ratio of the ion counts of the sublimation events at peak II and III in the aforementioned systems (Figures 5 & 6) is essentially constant at  $9 \pm 1:1$ . In conclusion, both higher temperature sublimation events II and III can be associated with isomer(s) of  $C_2H_3N$  along with the isotopically substituted counterparts.

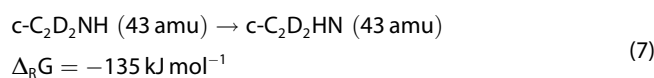
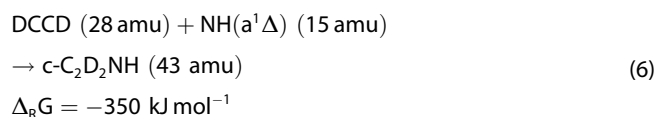
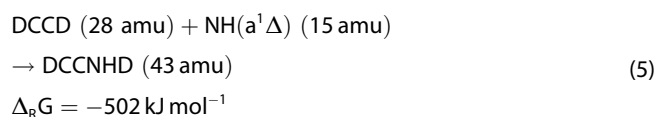
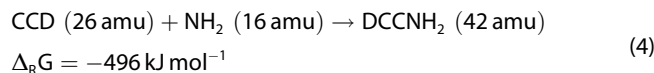
Having verified the formation and detection of the  $C_2H_3N$  isomer(s) via peaks II and III, it is pertinent to elucidate the nature of the isomer(s) formed (Figures 2 & 5). Recall that at 10.49 eV, only isomers **3** to **6** can be ionized. At 9.80 eV (Figure 5), sublimation event II remains unchanged, whereas peak III disappears. Therefore, this sublimation event must originate from isomer **3** (2H-azirine), which has an ionization energy above the photon energy of 9.80 eV, i.e. 9.97–10.04 eV. However, considering peak II at 9.80 eV, isomers **4–6** can still be ionized. A further reduction of the photon energy to 8.81 eV revealed no ion signal. Considering the ionization energies of isomers **4–6**, this indicates that peak II belongs to **4** (ethynamine). In summary, two isomers were detected via peaks II and III: **4** (ethynamine) and **3** (2H-azirine), respectively.

## 2.4. Reaction Mechanisms

Having identified the **4** (ethynamine) and **3** (2H-azirine) isomers, possible formation mechanisms must be proposed and verified. This is achieved by exposing  $C_2D_2/NH_3$  ices to 5 keV electrons at 10 nA for 5 min at a dose of  $0.042 \pm 0.007$  and  $0.029 \pm 0.005$  eV molecule $^{-1}$  for  $C_2D_2$  and  $NH_3$ , respectively. At these low doses isotopic scrambling of the reactants in low temperature ices can be excluded.<sup>[72]</sup> Experiments in pure ammonia ices revealed that upon interaction with energetic electrons, ammonia can decompose via atomic and molecular hydrogen loss, i.e. reactions (1) and (2), respectively, forming the amino ( $NH_2$ ) and imidogen species ( $NH(a^1\Delta)$ ). Detailed isotopic substitution experiments suggest that the atomic hydrogen loss channel dominates with fractions of about 90%.<sup>[73–74]</sup> Further, acetylene-d2 ( $C_2D_2$ ) undergoes carbon-hydrogen bond rupture upon interaction with energetic electrons to the ethynyl-d1 radical (CCD) plus atomic deuterium (reaction (3)).



In low temperature ices, doublet radicals can recombine if their recombination geometry is favorable.<sup>[37]</sup> This leads to the formation of **4** (ethynamine-d1) via reaction (4) (Figures 7 & 8). Likewise, imidogen ( $NH(a^1\Delta)$ ) may react with acetylene-d1 ( $C_2D_2$ ) via insertion into a carbon-deuterium bond (reaction (5)) to **4** (ethynamine-d2) or through addition to the carbon-carbon triple bond leading to 1H-azirine **6** ( $c-C_2D_2NH$ ) (reaction (6)), which may isomerize via hydrogen shift to 2H-azirine **3** ( $c-C_2D_2HN$ ) via a barrier of  $108 \text{ kJ mol}^{-1}$  (reaction (7)).



Alternatively, the amino radical ( $NH_2$ ) may add to the carbon-carbon triple bond of acetylene-d2 yielding a  $DCCDNH_2$  intermediate (7). This pathway is only open if the amino radical is in the vicinity of acetylene-d2 and if the amino radical has sufficient excess kinetic energy and/or vibrational energy to overcome the barrier of an additional  $16 \text{ kJ mol}^{-1}$ . As elucidated from the quantum chemical results, intermediate (7) may undergo multiple isomerizations via a hydrogen shift from the nitrogen to the terminal carbon atom to (8) followed by ring closure to (9). Also, these intermediates may undergo atomic hydrogen and/or deuterium loss yielding various  $C_2D_2HN$  (43 amu)/ $C_2DH_2N$  (42 amu) isotopologues and isotopomers.

The experiments in the  $C_2D_2/NH_3$  ices reveal that, at a photon energy of 9.80 eV, the signal at  $m/z = 42$  ( $C_2DH_2N^+$ ) dominates the signal at  $m/z = 43$  ( $C_2D_2HN^+$ ) with a greater intensity by a factor of  $5.8 \pm 0.8$ . The peak positions are in excellent agreement with peak II at  $m/z = 41$  ( $C_2H_3N^+$ ) in  $C_2H_2/NH_3$  ices for **4** (ethynamine) (Figure 9). Note that the lower signal level can be attributed to a lower irradiation dose and hence less reactive species produced in the low temperature ices. The detection of two isotopically labeled **4** species via  $m/z = m/z = 43$  ( $C_2D_2HN^+$ ) and  $42$  ( $C_2DH_2N^+$ ) suggests that **4** can be formed via reactions (4) and (5). It should be noted that these radical-radical reactions along with the insertion pathways of electronically excited species are in line with previous mechanistic investigations of processed interstellar analogue ices.<sup>[37]</sup> Methyl ( $CH_3$ ),<sup>[75]</sup> amino ( $NH_2$ ),<sup>[73–74]</sup> phosphino ( $PH_2$ ),<sup>[53,75]</sup> hydroxyl ( $OH$ ),<sup>[76–77]</sup> ethyl ( $C_2H_5$ ),<sup>[78]</sup> vinyl ( $C_2H_3$ ),<sup>[40,79]</sup> ethynyl ( $C_2H$ ),<sup>[40]</sup> formyl ( $HCO$ ),<sup>[80]</sup> hydroxycarbonyl ( $HOCO$ ),<sup>[81–84]</sup> hydroxymethyl

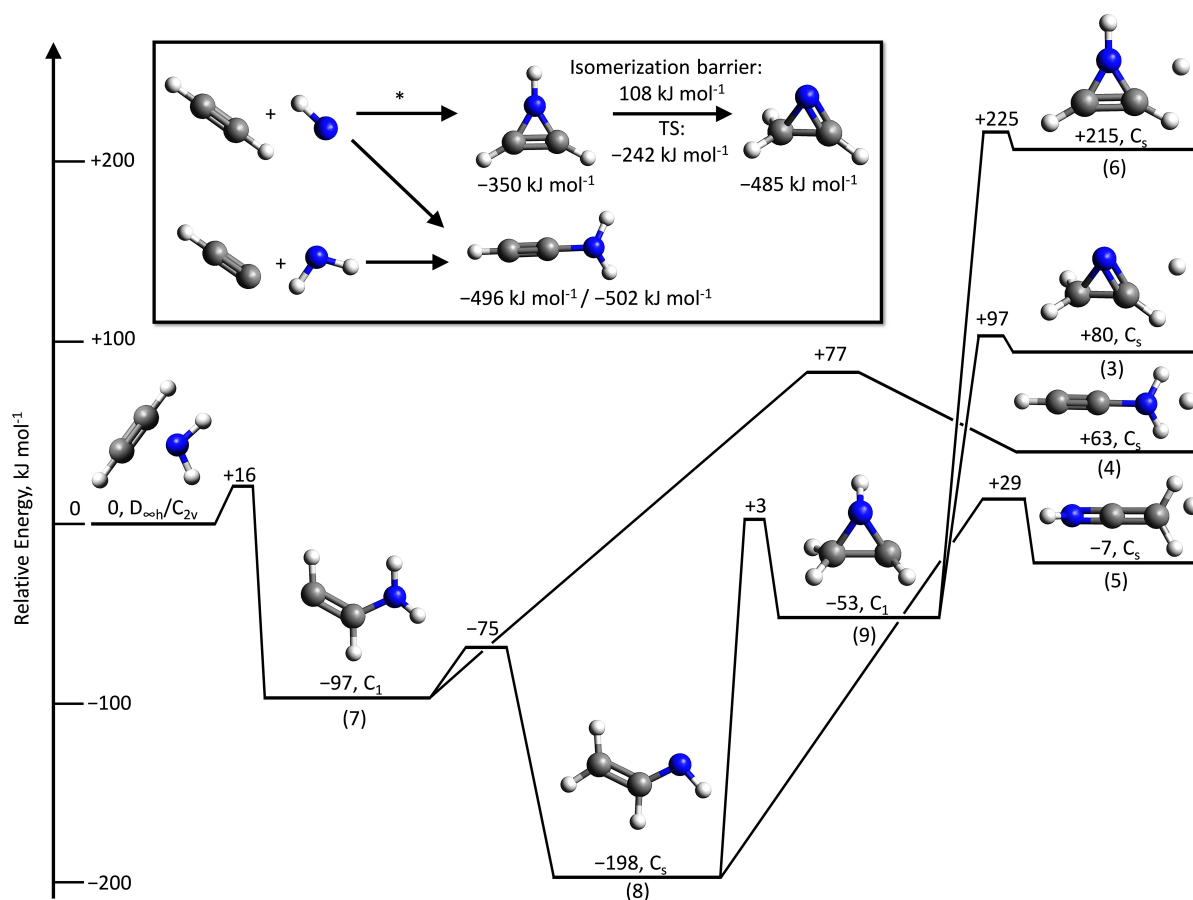


**Figure 7.** CCSD(T)/CBS + ZPVE reaction pathways of an amino radical ( $\text{NH}_2$ ) with acetylene ( $\text{C}_2\text{H}_2$ ). Inset: Calculated reaction energies of acetylene with imidogen ( $\text{NH}(a^1\Delta)$ , top) and an ethynyl radical ( $\text{CCH}$ ) with an amino radical (bottom). Along with the molecules displayed, coordinates for transition states can be found in Table S10.  $^* \text{C}_2\text{H}_2$  and  $\text{NH}(a^1\Delta)$  combine barrierlessly to an intermediate at  $-332 \text{ kJ mol}^{-1}$  (coordinates in Table S10), which then passes through a transition state at  $-268 \text{ kJ mol}^{-1}$  to form 1H-azirine (compound 6).

( $\text{CH}_2\text{OH}$ ),<sup>[85–86]</sup> methoxy ( $\text{CH}_3\text{O}$ ),<sup>[85–86]</sup> and acetyl ( $\text{CH}_3\text{CO}$ )<sup>[3,72]</sup> represent readily available reactants for radical-radical recombination within previously studied ices. Electronically excited reactants like carbene ( $\text{CH}_2$ ;  $a^1A_1$ ),<sup>[75]</sup> imidogen ( $\text{NH}$ ;  $a^1\Delta$ ),<sup>[73]</sup> and phosphinidene ( $\text{PH}$ ;  $a^1\Delta$ )<sup>[75]</sup> were found to insert into single bonds and also add to double and triple bonds. It should be noted that an initial addition of an amino radical ( $\text{NH}_2$ ) with excess kinetic and/or vibrational energy to the carbon-carbon triple bond of acetylene cannot be excluded based on the mass-to-charge ratio of the 4 (ethynamine-d1) product at  $m/z=42$  (Figure 8). Here, after passing a barrier with the addition of  $16 \text{ kJ mol}^{-1}$ , the doublet radical intermediate (7') could emit a deuterium atom leading to 4 (ethynamine-d1) in an overall endoergic reaction. This reaction energy could be incorporated by suprathermal amino radicals ( $\text{NH}_2$ ).

Finally, possible pathways for the formation of the detected 2H-azirine 3 ( $c\text{-C}_2\text{D}_2\text{HN}$ ) isomer should be noted. As stated above, addition of imidogen ( $\text{NH}(a^1\Delta)$ ) to the carbon-carbon triple bond may lead to 1H-azirine 6 ( $c\text{-C}_2\text{H}_2\text{NH}$ ), which was not detected in our experiment. However, the formation of 6 is exoergic by  $350 \text{ kJ mol}^{-1}$ .

Isomer 6 may react via two pathways. First, 6 can divert the internal vibrational energy to the surrounding matrix to stabilize. In this case, 6 would be detectable. Alternatively, if 6 is short lived, it could isomerize via hydrogen shift to 2H-azirine 3 ( $c\text{-C}_2\text{H}_3\text{N}$ ) via a barrier of  $108 \text{ kJ mol}^{-1}$  (reaction (7)). To be detectable, 3 has to be stabilized in the matrix. The potential energy surface (Figure 7) also demonstrates that 3 could form by the reaction of  $\text{C}_2\text{H}_2$  with a suprathermal amino radical ( $\text{NH}_2$ ) via intermediates 7, 8, and 9. However, the energetics indicates that if intermediate 8 forms, ketenimine 5 ( $\text{HNCCH}_2$ ) would also be an expected product. The lack of detection of 5 suggests that intermediate 8 does not form and the pathway to 3 from  $\text{C}_2\text{H}_2$  and  $\text{NH}_2$  is closed. Thus, our experimental findings propose that the reaction of imidogen ( $\text{NH}(a^1\Delta)$ ) with acetylene leads initially to 1H-azirine 6 ( $c\text{-C}_2\text{H}_2\text{NH}$ ), which undergoes hydrogen shift to 2H-azirine 3 ( $c\text{-C}_2\text{H}_3\text{N}$ ).

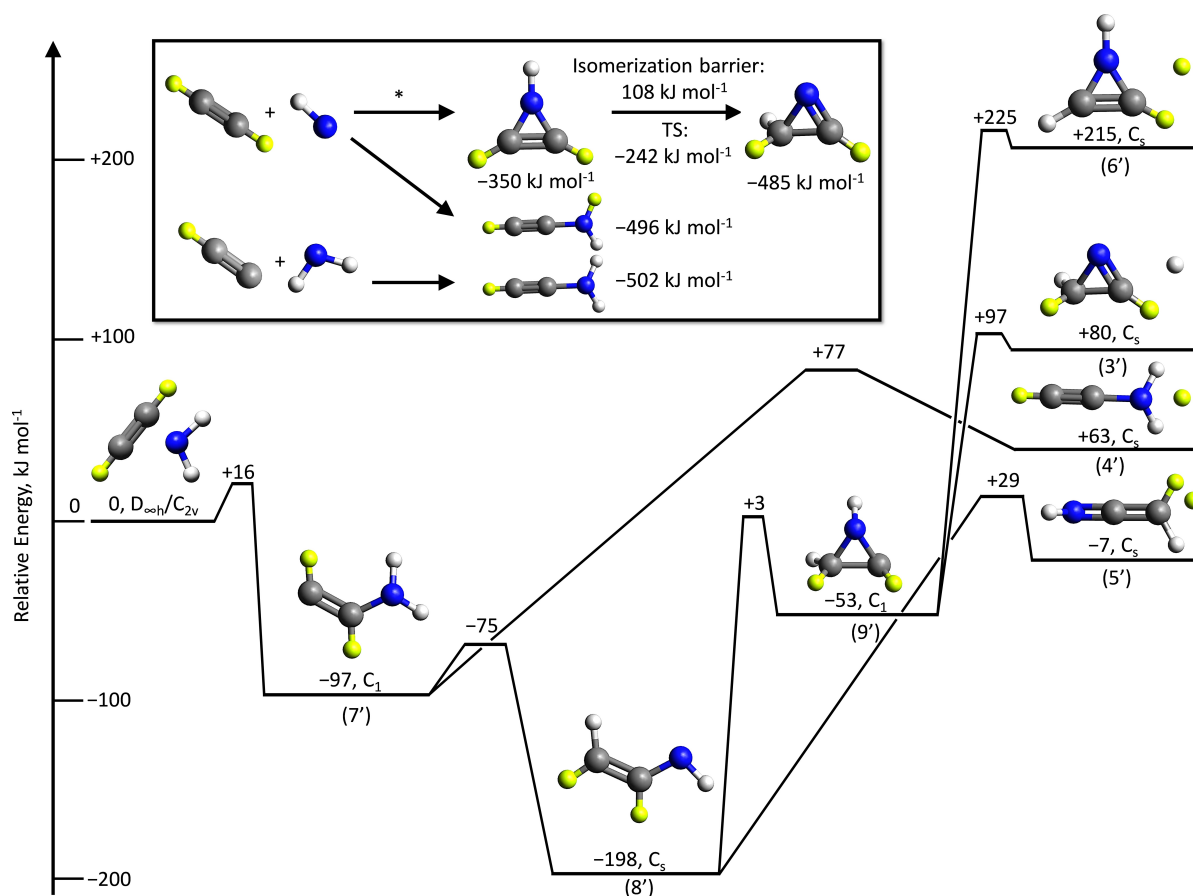


**Figure 8.** Calculated reaction pathways with energies based on the non-deuterated structures (Figure 7) of an amino radical ( $\text{NH}_2$ ) with acetylene-d2 ( $\text{C}_2\text{D}_2$ ). Deuterium atoms are labeled in yellow. Inset: Calculated reaction energies of acetylene-d2 with imidogen ( $\text{NH}(\text{a}^1\Delta)$ , top) and ethynyl-d1 ( $\text{CCD}$ ) with an amino radical (bottom).  $^*\text{C}_2\text{D}_2$  and  $\text{NH}(\text{a}^1\Delta)$  combine barrierlessly to an intermediate at  $-332 \text{ kJ mol}^{-1}$  (coordinates in Table S10), which then passes through a transition state at  $-268 \text{ kJ mol}^{-1}$  to form 1H-azirine (compound 6).

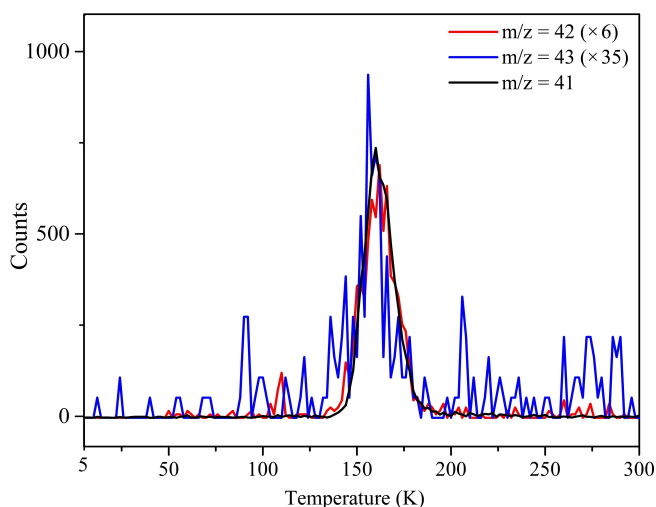


**Figure 9.** Temperature-programmed desorption profiles of the ionized neutral molecules at mass-to-charge ratios of 43 (red) and 42 (blue) subliming from  $\text{C}_2\text{D}_2\text{:NH}_3$  ice compared to the  $\text{C}_2\text{H}_2\text{:NH}_3$  ice at  $m/z = 41$  (black). Traces recorded for  $m/z = 42$  and  $43$  are scaled to  $m/z = 41$ .

### 3. Conclusions

Our combined experimental and computational investigation revealed the formation and detection of ethynamine (**4**;  $\text{HCCNH}_2$ ) and 2H-azirine (**3**;  $c\text{-C}_2\text{H}_3\text{N}$ ) in electron-irradiated ices of ammonia and acetylene. Studies with isotopically labeled reactants revealed two at least key pathways involving radical reactions through amino radicals ( $\text{NH}_2$ ) leading to **4** and addition processes of imidogen ( $\text{NH}$ ;  $\text{a}^1\Delta$ ) forming eventually **3**. The isomers were discriminated and identified upon sublimation of the processed ices and photoionizing the newly formed molecules by single photon ionization (PI) in the vacuum ultraviolet (VUV) range, which were mass resolved and detected within a reflectron time-of-flight mass spectrometer (ReTOF-MS). Radiolysis and photolysis of interstellar ices can convert methane ( $\text{CH}_4$ ) into acetylene ( $\text{C}_2\text{H}_2$ ),<sup>[41]</sup> and the latter could react with ammonia through non-equilibrium pathways as elucidated here to ethynamine **4** and 2H-azirine **3**. Upon sublimation in the hot core stage, both isomers could be detectable via radio telescopes such as the Atacama Large Millimeter/submillimeter Array (ALMA).

## Acknowledgements

Financial support from the US National Science Foundation (AST-1800975) to the University of Hawaii is greatly acknowledged. The experimental setup was financed by the W. M. Keck Foundation. RCF acknowledges funding from NASA Grant NNX17AH15G, startup funds provided by the University of Mississippi, and computer support provided by the Mississippi Center for Supercomputing Research which is, in turn, supported by the National Science Foundation grants CHE-1338056 and OIA-1757220.

## Conflict of Interest

The authors declare no conflict of interest.

**Keywords:** complex organic molecules · ionization potentials · IR spectroscopy · mass spectrometry · nonequilibrium processes

- [1] A. Bergantini, M. J. Abplanalp, P. Pokhilkov, A. I. Krylov, C. N. Shingledecker, E. Herbst, R. I. Kaiser, *Astrophys. J.* **2018**, *860*, 108, 101–115.
- [2] M. J. Abplanalp, R. Frigge, R. I. Kaiser, *Sci. Adv.* **2019**, *5*, eaaw5841.
- [3] N. F. Kleimeier, A. M. Turner, R. C. Fortenberry, R. I. Kaiser, *ChemPhysChem* **2020**, *21*, 1531–1540.
- [4] P. Solomon, K. Jefferts, A. Penzias, R. Wilson, *Astrophys. J.* **1971**, *168*, L107.
- [5] M. J. Abplanalp, S. Gozem, A. I. Krylov, C. N. Shingledecker, E. Herbst, R. I. Kaiser, *Proc. Natl. Acad. Sci. USA* **2016**, *113*, 7727–7732.
- [6] C. Zhu, R. Frigge, A. Bergantini, R. C. Fortenberry, R. I. Kaiser, *Astrophys. J.* **2019**, *881*, 156, 151–110.
- [7] M. J. Abplanalp, R. I. Kaiser, *Phys. Chem. Chem. Phys.* **2019**, *21*, 16949–16980.
- [8] A. J. Remijan, J. Hollis, F. J. Lovas, D. F. Plusquellic, P. Jewell, *Astrophys. J.* **2005**, *632*, 333.
- [9] Y. Liu, P. Guan, Y. Wang, L. Liu, J. Cao, *J. Phys. Chem. A* **2015**, *119*, 67–78.
- [10] T. Yamabe, M. Kaminoyama, T. Minato, K. Hori, K. Isomura, H. Taniguchi, *Tetrahedron* **1984**, *40*, 2095–2099.
- [11] M. Bogey, J.-L. Destombes, J.-M. Denis, J.-C. Guillemin, *J. Mol. Spectrosc.* **1986**, *115*, 1–14.
- [12] T. Takayanagi, Y. Kurosaki, K. Sato, S. Tsunashima, *J. Phys. Chem. A* **1998**, *102*, 10391–10398.
- [13] A. G. Császár, J. Demaison, H. D. Rudolph, *J. Phys. Chem. A* **2015**, *119*, 1731–1746.
- [14] C. E. Dickerson, P. P. Bera, T. J. Lee, *J. Phys. Chem. A* **2018**, *122*, 8898–8904.
- [15] T. V.-T. Mai, L. K. Huynh, *Phys. Chem. Chem. Phys.* **2019**, *21*, 17232–17239.
- [16] X. Yang, S. Maeda, K. Ohno, *J. Phys. Chem. A* **2005**, *109*, 7319–7328.
- [17] B. J. Smith, L. Radom, *J. Am. Chem. Soc.* **1992**, *114*, 36–41.
- [18] M. Jablonski, T. M. Krygowski, *ChemPhysChem* **2020**.
- [19] P. M. Mayer, M. S. Taylor, M. W. Wong, L. Radom, *J. Phys. Chem. A* **1998**, *102*, 7074–7080.
- [20] M. E. Jacox, D. E. Milligan, *J. Am. Chem. Soc.* **1963**, *85*, 278–282.
- [21] S. Zavoruev, R.-I. Rakauskas, *Theo. Exp. Chem.* **1990**, *25*, 445–450.
- [22] A. Padwa, *Acc. Chem. Res.* **1976**, *9*, 371–378.
- [23] A. F. Khlebnikov, M. S. Novikov, *Tetrahedron* **2013**, *69*, 3363–3401.
- [24] A. F. Khlebnikov, M. S. Novikov, N. V. Rostovskii, *Tetrahedron* **2019**, *75*, 2555–2624.
- [25] M. J. Alves, F. T. Costa, in *Heterocyclic Targets in Advanced Organic Synthesis* (Eds.: M. d. C. Carreiras, J. Marco-Contelles), **2011**, pp. 145–172.
- [26] A. Padwa, C. Murphree, in *Progress in Heterocyclic Chemistry*, Vol. 15, Elsevier, **2003**, pp. 75–99.
- [27] A. Padwa, in *Advances in Heterocyclic Chemistry*, Vol. 99, Elsevier, **2010**, pp. 1–31.
- [28] H. Zhou, M.-H. Shen, H.-D. Xu, *Synlett* **2016**, *27*, 2171–2177.
- [29] C. Bornemann, M. Klessinger, *Chem. Phys.* **2000**, *259*, 263–271.
- [30] J.-C. Guillemin, J.-M. Denis, M.-C. Lasne, J.-L. Ripoll, *Tetrahedron* **1988**, *44*, 4447–4455.
- [31] H. Bock, R. Dammel, S. Aygen, *J. Am. Chem. Soc.* **1983**, *105*, 7681–7685.
- [32] H.-G. Cho, *Bull. Korean Chem. Soc.* **2014**, *35*, 2093–2096.
- [33] N. Balucani, D. Skouteris, F. Leonori, R. Petrucci, M. Hamberg, W. D. Geppert, P. Casavecchia, M. Rosi, *J. Phys. Chem. A* **2012**, *116*, 10467–10479.
- [34] S.-H. Lee, C.-H. Chin, W.-K. Chen, W.-J. Huang, C.-C. Hsieh, *Phys. Chem. Chem. Phys.* **2011**, *13*, 8515–8525.
- [35] C. Wentrup, H. Briehl, P. Lorencak, U. J. Vogelbacher, H. W. Winter, A. Maquestiau, R. Flammang, *J. Am. Chem. Soc.* **1988**, *110*, 1337–1343.
- [36] P. Lu, Y. Wang, *Chem. Soc. Rev.* **2012**, *41*, 5687–5705.
- [37] A. M. Turner, R. I. Kaiser, *Acc. Chem. Res.* **2020**, *53*, 2791–2805.
- [38] C. Zhu, A. M. Turner, M. J. Abplanalp, R. I. Kaiser, *Astrophys. J. Suppl. Ser.* **2018**, *234*, 15, 11–13.
- [39] B. M. Jones, R. I. Kaiser, *J. Phys. Chem. Lett.* **2013**, 1965–1971.
- [40] M. J. Abplanalp, S. Góbi, R. I. Kaiser, *Phys. Chem. Chem. Phys.* **2019**, *21*, 5378–5393.
- [41] M. J. Abplanalp, B. M. Jones, R. I. Kaiser, *Phys. Chem. Chem. Phys.* **2018**, *20*, 5435–5468.
- [42] A. A. Boogert, P. A. Gerakines, D. C. Whittet, *Annu. Rev. Astron. Astrophys.* **2015**, *53*.
- [43] J. M. Greenberg, C. Van de Bult, L. J. Allamandola, *J. Phys. Chem.* **1983**, *87*, 4243–4260.
- [44] E. L. Gibb, D. C. B. Whittet, A. C. A. Boogert, A. G. G. M. Tielens, *Astrophys. J. Suppl. Ser.* **2004**, *151*, 35–73.
- [45] A. J. Verbitser, D. E. Peterson, M. F. Skrutskie, M. Cushing, P. Helfenstein, M. J. Nelson, J. Smith, J. C. Wilson, *Icarus* **2006**, *182*, 211–223.
- [46] J. Emery, D. Burr, D. Cruikshank, R. H. Brown, J. Dalton, *Astron. Astrophys.* **2005**, *435*, 353–362.
- [47] J. M. Bauer, T. L. Roush, T. R. Geballe, K. J. Meech, T. C. Owen, W. D. Vacca, J. T. Rayner, K. T. Jim, *Icarus* **2002**, *158*, 178–190.
- [48] M. E. Brown, W. M. Calvin, *Science* **2000**, *287*, 107–109.
- [49] C. Dumas, R. J. Terrile, R. H. Brown, G. Schneider, B. A. Smith, *Astron. J.* **2001**, *121*, 1163.
- [50] D. C. Jewitt, J. Luu, *Nature* **2004**, *432*, 731–733.
- [51] M. J. Abplanalp, M. Förstel, R. I. Kaiser, *Chem. Phys. Lett.* **2016**, *644*, 79–98.
- [52] O. S. Heavens, *Optical Properties of Thin Solid Films*, Butterworths Scientific Publications, **1955**.
- [53] A. M. Turner, M. J. Abplanalp, S. Y. Chen, Y. T. Chen, A. H. Chang, R. I. Kaiser, *Phys. Chem. Chem. Phys.* **2015**, *17*, 27281–27291.
- [54] M. Satorre, J. Leliwa-Kopystynski, C. Santonja, R. Luna, *Icarus* **2013**, *225*, 703–708.
- [55] R. Hudson, R. Ferrante, M. Moore, *Icarus* **2014**, *228*, 276–287.
- [56] M. J. Abplanalp, R. I. Kaiser, *Astrophys. J.* **2020**, *889*, 3, 1–26.
- [57] M. Bouilloud, N. Fray, Y. Bénilan, H. Cottin, M.-C. Gazeau, A. Jolly, *Mon. Not. R. Astron. Soc.* **2015**, *451*, 2145–2160.
- [58] P. Hovington, D. Drouin, R. Gauvin, *Scanning* **1997**, *19*, 1–14.
- [59] W. A. VonDrasek, S. Okajima, J. P. Hessler, *Appl. Opt.* **1988**, *27*, 4057–4061.
- [60] S. Maity, R. I. Kaiser, B. M. Jones, *Faraday Discuss.* **2014**, *168*, 485–516.
- [61] K. Raghavachari, G. W. Trucks, J. A. Pople, M. Head-Gordon, *Chem. Phys. Lett.* **1989**, *157*, 479–483.
- [62] R. A. Kendall, T. H. Dunning Jr, R. J. Harrison, *J. Chem. Phys.* **1992**, *96*, 6796–6806.
- [63] K. A. Peterson, T. H. Dunning Jr, *J. Chem. Phys.* **1995**, *102*, 2032–2041.
- [64] J. M. Martin, T. J. Lee, *Chem. Phys. Lett.* **1996**, *258*, 136–143.
- [65] A. D. Becke, *J. Chem. Phys.* **1993**, *98*, 5648–5652.
- [66] C. Lee, W. Yang, R. G. Parr, *Phys. Rev. B* **1988**, *37*, 785.
- [67] W. Yang, R. G. Parr, C. Lee, *Phys. Rev. A* **1986**, *34*, 586.
- [68] H. Werner, P. J. Knowles, G. Knizia, F. Manby, M. Schütz, P. Celani, W. Györfy, D. Kats, T. Korona, R. Lindh, MOLPRO, version 2015.1, a package of ab initio programs, University of Cardiff Chemistry Consultants (UC3): Cardiff, Wales, UK **2015**.
- [69] H. J. Werner, P. J. Knowles, G. Knizia, F. R. Manby, M. Schütz, *WIREs Comput. Mol. Sci.* **2012**, *2*, 242–253.
- [70] M. Frisch, G. Trucks, H. Schlegel, G. Scuseria, M. Robb, J. Cheeseman, G. Scalmani, V. Barone, B. Mennucci, G. Petersson, *Gaussian, Inc* **2009**, Wallingford, CT.
- [71] S. K. Singh, T.-Y. Tsai, B.-J. Sun, A. H. Chang, A. M. Mebel, R. I. Kaiser, *J. Phys. Chem. Lett.* **2020**, *11*, 5383–5389.
- [72] N. F. Kleimeier, A. K. Eckhardt, R. I. Kaiser, *Astrophys. J.* **2020**, *901*, 84, 81–11.

- [73] M. Förstel, Y. A. Tsegaw, P. Maksyutenko, A. M. Mebel, W. Sander, R. I. Kaiser, *ChemPhysChem* **2016**, *17*, 2726–2735.
- [74] M. Förstel, P. Maksyutenko, B. M. Jones, B.-J. Sun, S.-H. Chen, A. Chang, R. I. Kaiser, *ChemPhysChem* **2015**, *16*, 3139–3142.
- [75] A. M. Turner, M. J. Abplanalp, R. I. Kaiser, *Astrophys. J.* **2016**, *819*, 97, 91–15.
- [76] A. Bergantini, P. Maksyutenko, R. I. Kaiser, *Astrophys. J.* **2017**, *841*, 96, 91–24.
- [77] A. M. Turner, A. S. Koutsogiannis, N. F. Kleimeier, A. Bergantini, C. Zhu, R. C. Fortenberry, R. I. Kaiser, *Astrophys. J.* **2020**, *896*, 88, 81–89.
- [78] M. J. Abplanalp, R. I. Kaiser, *Astrophys. J.* **2016**, *827*, 132, 131–129.
- [79] L. Zhou, S. Maity, M. Abplanalp, A. Turner, R. I. Kaiser, *Astrophys. J.* **2014**, *790*.
- [80] R. Frigge, C. Zhu, A. M. Turner, M. J. Abplanalp, B.-J. Sun, Y.-S. Huang, A. H. Chang, R. I. Kaiser, *Chem. Commun.* **2018**, *54*, 10152–10155.
- [81] B. M. McMurtry, A. M. Turner, S. E. Saito, R. I. Kaiser, *Chem. Phys.* **2016**, *472*, 173–184.
- [82] A. K. Eckhardt, A. Bergantini, S. K. Singh, P. R. Schreiner, R. I. Kaiser, *Angew. Chem. Int. Ed.* **2019**, *58*, 5663–5667.
- [83] C. Zhu, A. M. Turner, C. Meinert, R. I. Kaiser, *Astrophys. J.* **2020**, *889*, 134, 131–110.
- [84] B. M. McMurtry, S. E. Saito, A. M. Turner, H. K. Chakravarty, R. I. Kaiser, *Astrophys. J.* **2016**, *831*, 174.
- [85] S. Maity, R. I. Kaiser, B. M. Jones, *Phys. Chem. Chem. Phys.* **2015**, *17*, 3081–3114.
- [86] A. Bergantini, S. Góbi, M. J. Abplanalp, R. I. Kaiser, *Astrophys. J.* **2018**, *852*, 70, 71–13.

---

Manuscript received: January 28, 2021

Revised manuscript received: March 23, 2021

Accepted manuscript online: April 1, 2021

Version of record online: April 19, 2021